

ORIGINAL ARTICLE

Subcycle control of terahertz waveform polarization using all-optically induced transient metamaterials

N Kamaraju^{1,2}, Andrea Rubano^{1,3}, Linke Jian⁴, Surajit Saha⁴, T Venkatesan⁴, Jan Nötzold¹, R Kramer Campen¹, Martin Wolf¹ and Tobias Kampfrath¹

Coherent radiation with frequencies ranging from 0.3 to 30 THz has recently become accessible using femtosecond laser technology. These terahertz (THz) waves have already been applied in spectroscopy and imaging and can be manipulated using static optical elements such as lenses, polarizers and filters. However, ultrafast modulation of THz radiation is required as well, for instance, in short-range wireless communication or for preparing shaped THz transients for the coherent control of numerous material excitations. Here, we demonstrate an all-optically created transient metamaterial that allows us to manipulate the polarization of THz waveforms with subcycle switch-on times. The polarization-modulated pulses are potentially interesting for controlling elementary motions such as the vibration of crystal lattices, the rotation of molecules and the precession of spins.

Light: Science & Applications (2014) 3, e155; doi:10.1038/lisa.2014.36; published online 28 February 2014

Keywords: terahertz metamaterial; terahertz optics; terahertz polarization control

INTRODUCTION

Today, coherent electromagnetic transients covering the terahertz (THz) frequency window can routinely be generated and detected using femtosecond laser technology.¹ Such THz pulses have numerous applications, such as the probing² and even control³ of fundamental modes, for example, the vibrations of molecules and crystals or spin precessions in solids. In addition, THz radiation has proven to be an excellent tool in non-destructive and material-specific imaging⁴ and is under consideration as an information carrier in short-range wireless communication at THz bit rates, thereby potentially replacing slower current gigahertz-based technology.⁵ Such applications heavily rely on the manipulation of THz radiation,⁶ and static elements such as lenses, waveplates and frequency filters are readily available.⁷ However, the dynamic manipulation of THz transients with subcycle precision is required, as well in fields such as THz telecommunication (where information must be imprinted on a pulse train⁵) and THz coherent control over matter (where tailored waveforms have been predicted to drive, for instance, the configuration of a crystal lattice along a desired path⁸).

To date, ultrafast THz switches and modulators have been demonstrated based on photonic materials with enhanced light–matter interaction.^{9–17} Examples of these microstructures are metamaterials, artificial plane metallic structures on an insulating substrate with a period much smaller than the vacuum wavelength of the THz radiation (300 μm at 1 THz). Metamaterials have an effective refractive index that can be tuned by tailoring the shape of the metal structure. Ultrafast switching is triggered by photodoping the underlying semiconductor

substrate using a femtosecond laser pulse, thereby modifying its refractive index. However, apart from such global modulation, the geometry of the metal structure is difficult to change, and the use of only two materials (the metal and substrate) does not allow for a gradual spatial variation of the refractive index.

A more flexible approach is to start with a homogeneous substrate into which the photonic structure is all-optically imprinted,^{18–21} for example, using the scheme presented in Figure 1a. Here, a laser beam with a spatially modulated cross-section is incident to a plane substrate, in which the optical intensity pattern is translated into a spatial modulation of the refractive index. Compared with standard lithography, such ‘gray-scale transient lithography’ offers improved flexibility. First, when combined with a freely programmable spatial light modulator,¹⁹ the transverse modulation of the pump beam can be changed fully and easily. Second, one can realize a continuous variation of the optical permittivity, even on ultrafast time scales. To date, this scheme has been used to imprint transient gratings with a period on the order of the probing wavelength, which permitted the partial diffraction of an incident infrared¹⁸ and THz pulse^{19,20} into a surface-type or free-space wave. However, fascinating applications of gray-scale transient lithography, for instance, transient metamaterials and arbitrary on-the-fly manipulation of THz fields, have been largely unexplored.

In this report, we demonstrate the ultrafast all-optical generation of a transient wire-grid polarizer (WGP), a textbook example of an anisotropic metamaterial, and its use in the manipulation of the polarization state of THz transients with subcycle switch-on times. The

¹Fritz Haber Institute of the Max Planck Society, 14195 Berlin, Germany; ²Department of Electrical, Computer, and Systems Engineering, Rensselaer Polytechnic Institute, Troy, NY 12180, USA; ³CNR-SPIN, Dipartimento di Fisica, Università di Napoli Federico II, Napoli, Italy and ⁴NUSNNI-Nanocore, National University of Singapore, Singapore
Correspondence: Dr N Kamaraju, Department of Electrical, Computer, and Systems Engineering, Rensselaer Polytechnic Institute, Troy, NY 12180, USA
E-mail: nkamaraju@gmail.com

Or Dr T Kampfrath, Fritz Haber Institute of the Max Planck Society, Faradayweg 4–6, 14195 Berlin, Germany
E-mail: kampfrath@fhi-berlin.mpg.de

Received 26 July 2013; revised 18 October 2013; accepted 13 November 2013

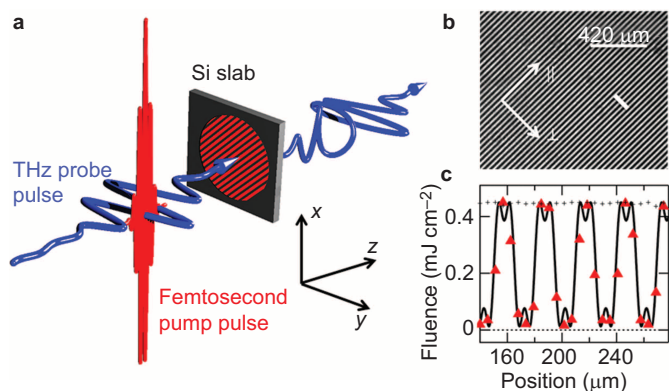


Figure 1 Scheme of a transient metamaterial induced by femtosecond gray-scale lithography. **(a)** A femtosecond laser pulse with a tailored beam cross-section generates an electron–hole plasma with a spatially varying density in a Si slab, thereby inducing a refractive-index modulation ranging from metallic to dielectric. The transient optical properties are probed using a time-delayed THz pulse. **(b)** Intensity distribution of the pump-beam cross-section at the slab plane as obtained by imaging a striped shadow mask. **(c)** Red symbols are the result of a scan along the white line in **b**, and the solid line is a calculation based on a plane-wave expansion (Supplementary Information S3). The periodic pattern is expected to instantaneously induce a transient wire-grid polarizer that can be used to manipulate the polarization of a THz transient on a subcycle scale **(a)**. Part of the unshaped (homogeneous) beam profile is also shown (black + symbols). THz, terahertz.

potential applications of this approach include ultrafast pulse splitters and polarization multiplexers, which are, for example, required in THz wireless communication technology. Moreover, the scheme can straightforwardly be extended to implement all varieties of transient THz photonic devices, such as lenses, filters and waveplates, thereby offering significantly more flexibility than previous demonstrations of THz modulators that employed lithographically fabricated metamaterials.^{11–16}

MATERIALS AND METHODS

Gray-scale transient lithography

As illustrated in Figure 1a, we irradiate a semiconductor slab with an optical femtosecond laser pulse whose transverse beam profile is shaped by a shadow mask. Through light absorption in the semiconductor, the beam pattern is translated into a spatial density distribution of an electron–hole plasma and thus, a refractive-index distribution $n(x,y,z,\omega)$ in the slab: the irradiated points (x,y,z) become metallic (the real part of the permittivity n^2 is negative), whereas the dark areas remain dielectric ($\text{Re } n^2 > 0$). The effect of the photoinduced charge carriers is more pronounced at lower frequencies $\omega/2\pi$ because their permittivity is roughly proportional to the pump intensity times $1/\omega^2$ (Supplementary Fig. S1). Because features much smaller than the THz wavelength can be realized with optical radiation, we can ‘switch on’ a tailored metamaterial for THz radiation on the femtosecond time scale. The anisotropic transmittance of this dynamic structure is probed using a THz pulse arriving at a variable delay after the pump pulse. By temporally overlapping the pump and the probe beam, we are even able to manipulate the THz transient with subcycle precision (Figure 1a).

As an initial demonstration of our ability to manipulate THz transients on a subcycle level, we create a WGP composed of a periodic array of parallel metal wires. This pattern is realized by imaging a shadow mask with a periodic arrangement of adjacent fully transparent and absorbing stripes onto an insulating Si slab (Figure 1a).

Set-up details

We employ intense femtosecond laser pulses (40 fs duration, 800 nm center wavelength, 7 mJ pulse energy, 1 kHz repetition rate). A small fraction of the energy per pulse is used to generate THz pulses by optical rectification in ZnTe(110) crystals (0.5 mm thickness),^{1,2} while the majority of the laser beam (1 cm diameter) is directed through a glass substrate, on top of which an array of Cr wires (103 nm thickness, 15 μm width, 30 μm period) is fabricated using optical lithography. This shadow-mask pattern is imaged onto a high-resistivity (approximately 20 $\Omega\text{ cm}$) Si slab (10 μm thickness) using a 4*f* imaging set-up (as detailed in Supplementary Information S3). The resulting transient WGP is probed using a time-delayed THz pulse that travels collinearly with the pump beam after reflection off a pump-transparent glass plate with an indium-tin oxide coating. The THz electric field is subsequently detected by electrooptic sampling,^{1,2} and the various polarization configurations (\parallel and \perp) are covered by appropriately rotating the shadow mask and a THz polarizer before and after the Si slab.

Excitation profile

The pump beam intensity profile in the slab plane is measured using a charge-coupled device and is presented in Figure 1b and 1c. The distance between the centers of adjacent stripes (30 μm) is substantially smaller than the THz wavelength inside Si (88 μm at 1 THz) and the slab thickness. Thus, we expect that our transient WGP acts as an effective homogeneous anisotropic medium whose optical properties are fully determined by the refractive index along its symmetry axes.

We tested this expectation by calculating the pump intensity profile using a plane-wave expansion (Supplementary Information S3). These calculations not only reproduce the measured profile well (Figure 1c), but also verify that the shape of this distribution persists over the entire thickness of the Si slab (Supplementary Fig. S3a). In addition, the calculations reveal two minor effects, namely, some modulation along the propagation direction arising from pump depletion and a standing wave close to the backside of the slab. Because the slab is much thinner than the THz wavelength, this z dependence can be summarized in an effective z -independent refractive index $n(x,y,\omega)$ (Supplementary Information S3). Note that the pump intensity pattern (Figure 1c) is not as perfectly square-type as the shadow mask, which is a result of the 12- μm -wide point spread function of our 4*f* imaging system.

In Si, the pump-induced change in the refractive index proceeds in a temporally step-like manner, with a rise time of several 100 fs.²² Subsequent relaxation and diffusion of the electron–hole pairs proceeds on time scales of nanoseconds²² and 100 ps (over a distance of 1 μm),^{23,24} respectively. These slower processes do not play a role on the time and length scales relevant to this experiment.

RESULTS AND DISCUSSION

Wire-grid polarizer theory

When the THz probe pulse is polarized parallel (\parallel) to the wires, the free charge carriers inside the metallic parts are moved in the same manner as for a plane metal surface. Likewise, the substrate parts between wires respond in the same manner as an extended dielectric slab. This configuration can be considered as a parallel connection of electric resistors, and the effective refractive index n_{\parallel} for this configuration is given by the relation²⁵

$$n_{\parallel}^2(\omega) = \langle n^2(x,y,\omega) \rangle \quad (1)$$

where $\langle \cdot \rangle$ denotes averaging along the in-plane direction perpendicular to the wires.

The situation changes drastically when the incident THz radiation is polarized perpendicular (\perp) to the wires. In this case, the charge carriers will be shifted toward the wire surface, which leads to the build-up of an electric field that partially compensates for the driving field inside the wire. Consequently, much less charge than for parallel polarization will be translated, implying less reflection of the incident light. This configuration can be considered as a series connection of resistors, and the effective refractive index n_{\perp} for this configuration is determined by²⁵

$$\frac{1}{n_{\perp}^2(\omega)} = \left\langle \frac{1}{n^2(x,y,\omega)} \right\rangle \quad (2)$$

Homogeneous pump profile

The electromagnetic properties of the WGP are measured by broadband THz probe pulses polarized either along the \parallel or \perp direction (Figure 1a). As a reference, Figure 2a shows the transient electric field $E_{UE}(t)$ of a THz pulse detected after having traversed an unexcited (UE) silicon slab. When the slab is illuminated with a femtosecond laser pulse with a homogeneous beam profile (Figure 1c) approximately 60 ps before the arrival of the probe pulse, we observe that the THz field amplitude undergoes a reduction by one order of magnitude (Figure 2b). This decrease predominantly arises from the large reflectance (rather than the absorption) of the transiently metallized Si slab, which is observed to increase from 53% for an unexcited slab to 86% at 1 THz (Supplementary Fig. S2).

Transient wire-grid polarizer

It is interesting to observe the effect of replacing the homogeneous pump-beam profile with the striped structure of Figure 1b. When the stripes are parallel (\parallel) to the THz polarization, we obtain a waveform (Figure 2c) whose overall amplitude is a factor of approximately 2 larger than that observed for homogeneous excitation (Figure 2b). This rescaling effect is plausible because the effectively excited Si

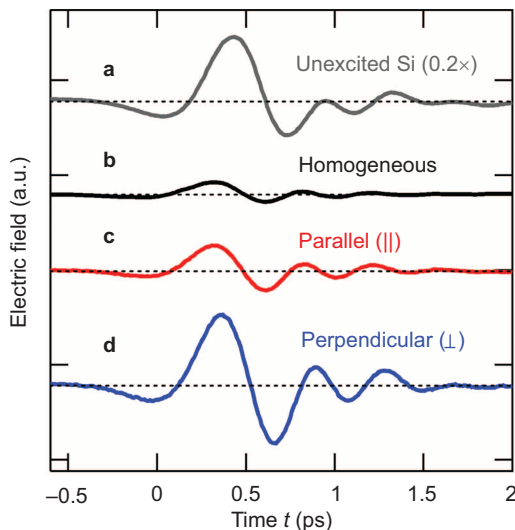


Figure 2 Time-domain characterization of the transient wire-grid polarizer. (a) Transient electric field of a THz pulse that has traversed an Si slab without excitation. (b) 60 ps after homogeneous excitation with an 800 nm pump pulse. (c) 60 ps after excitation with the pattern of Figure 1b with the THz polarization parallel. (d) Perpendicular to the wire orientation. The different amplitude and phase shift of the waveforms in **c** and **d** are a clear signature of the highly anisotropic response of the transient metamaterial. THz, terahertz.

volume fraction has been reduced by approximately the same factor (Figure 1c). Note, however, the strikingly different behavior when the stripe direction is perpendicular (\perp) to the THz polarization. In this case, the field amplitude is a factor of approximately 3 larger than for the \parallel configuration (Figure 2d). In other words, the transient structure indeed acts like a polarizer with a power extinction ratio on the order of 10.

The highly anisotropic response of the transient metamaterial can be studied further in the frequency domain: Figure 3a displays the power transmittance $|E_{\perp}(\omega)/E_{UE}(\omega)|^2$ and $|E_{\parallel}(\omega)/E_{UE}(\omega)|^2$, that is, the intensity spectrum of the respective perpendicular and parallel component divided by the spectrum of the unexcited slab. While the \parallel transmittance is observed to increase monotonically with frequency, its \perp counterpart exhibits a broad maximum. In addition, we observe that the transmittance of the transient WGP is significantly larger for perpendicular than for parallel polarization, reaching an extinction ratio $|E_{\perp}(\omega)/E_{\parallel}(\omega)|^2$ of greater than 10 near $\omega/2\pi = 1.5$ THz (Figure 3a), consistent with our time-domain observations (Figure 2). Notably, the \parallel component is observed to exhibit a larger negative, more metal-like phase shift than the \perp component (Figure 3b). Therefore, our transient WGP can also be used as a retardation plate.

Comparison to effective-medium model

To demonstrate that the photoexcited slab can indeed be considered a birefringent THz metamaterial, we calculate the refractive indices $n_{\perp}(\omega)$ and $n_{\parallel}(\omega)$ using effective-medium theory²⁵ (Equations (1) and (2)). The refractive-index distribution $n(x,y,\omega)$ is obtained from the pump intensity distribution (Figure 1c) and transmission measurements of the Si slab following excitation with a homogeneous pump beam at various pulse energies (Figure 2b and Supplementary

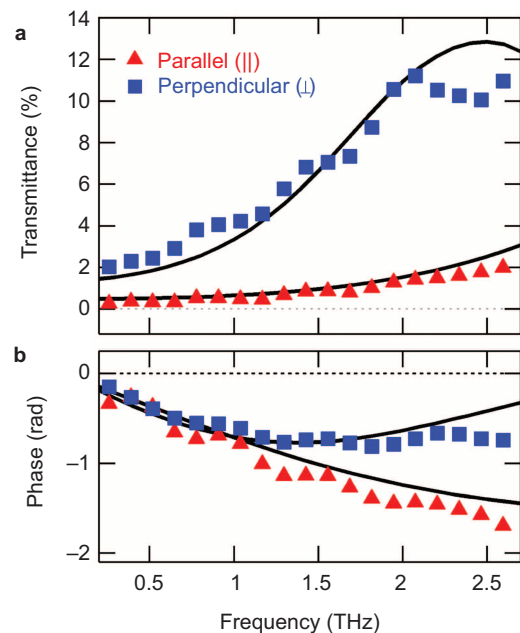


Figure 3 Spectral transmittance of the transient wire-grid polarizer. (a) Power transmittance of the Si slab 60 ps after excitation with the pump intensity pattern of Figure 1b, referenced to the unexcited slab. The spectra demonstrate that the transient structure acts as a polarizer. (b) Spectral phase shift, revealing the more metallic behavior (negative phase shift) of the structure for THz radiation polarized parallel to the transient wires. Solid lines are model calculations based on effective-medium theory, without using any fit parameters. THz, terahertz.

Information S1). Using $n_{\perp}(\omega)$ and $n_{\parallel}(\omega)$, the transmission coefficients of the slab are calculated using standard formulas (Supplementary Information S1, Equation (S1)) that also account for all the reflections occurring at the Si/air interfaces.²⁶ The modulus and phase of the calculated transmission coefficients are shown by the solid lines in Figure 3a and 3b, respectively. We observe excellent agreement between experiment and theory, both in terms of magnitude and trend, without invoking any fitting parameters. This agreement extends to frequencies of approximately 2.5 THz, at which the metamaterial condition (periodicity much smaller than wavelength inside the medium) is no longer met. We summarize that our modeling corroborates the notion that we have successfully and all-optically created a transient metamaterial.

While our experiment provides a first proof-of-principle of a photoinduced metamaterial, our model allows us to predict the performance of the WGP under modified conditions. In particular, calculations indicate that a substantially enhanced extinction ratio (as high as 4000 at 0.6 THz), an enhanced relative \parallel -transmittance (greater than 100%) and an increased bandwidth could be achieved by cooling the Si slab to cryogenic temperatures (thereby reducing THz losses arising from Drude absorption²⁷) and by increasing the contrast between the dark and bright regions of the pump intensity pattern (Supplementary Fig. S4). Finally, an ultrafast ‘switch-off’ of the structure can be realized with appropriate materials such as oxygen-doped Si.²⁸

Ultrafast polarization manipulation

As our metamaterial is generated on a time scale of approximately 100 fs, it offers the fascinating possibility for subcycle polarization manipulation of THz transients. The results of such an experiment are presented in Figure 4. A THz pulse, polarized along y and thus at 45° with respect to the WGP major axes, is incident onto the still unexcited Si slab (Figure 1a). Once part of the transient has traversed the Si, the pump pulse imprints the WGP structure; thus, the \parallel and \perp components of the remaining THz transient experience a different

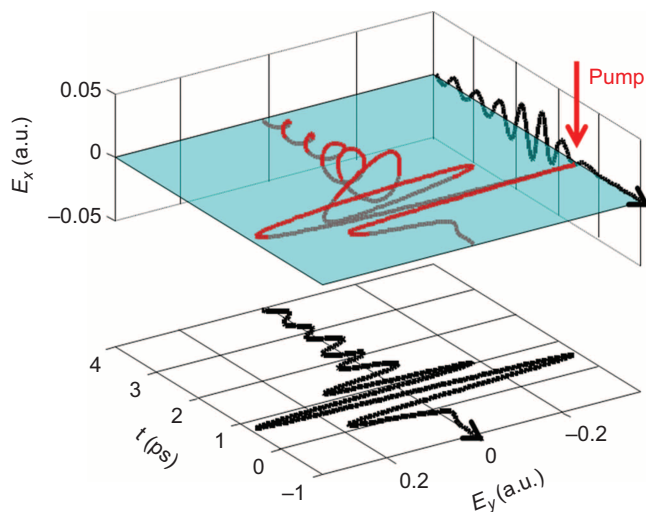


Figure 4 Experimental demonstration of subcycle polarization manipulation of a THz waveform. The graph displays the measured transient electric field of a THz waveform after interaction with a time-dependent metamaterial (Figure 1a). After the leading part of the THz pulse has traversed an unexcited Si slab, the transient wire-grid polarizer is switched on, which permits the polarization of the trailing part to be changed from linear to elliptical. The units of E_x and E_y are the same. THz, terahertz.

attenuation and phase shift, resulting in an elliptically polarized trailing part of the THz pulse. Note that the switched part of the transient $E_x(t)$ is substantially shorter than the incident THz pulse, which suggests that the ultrafast metamaterial could also be used as a pulse cutter or a device to broaden the spectrum of THz pulses.

CONCLUSIONS

We have provided a first experimental demonstration of an all-optically induced THz metamaterial that can be switched on femtosecond time scales and thus, permits the manipulation of THz transients with subcycle resolution. The polarization-modulated pulses are potentially interesting for controlling elementary motions such as lattice vibrations,^{8,29} molecular rotations³⁰ and spin precession.³¹ Future work will employ programmable spatial light modulators¹⁹ to realize other types of microstructures that will enable the further manipulation of THz light, such as frequency shifting³² and spectral lensing.²³ In addition, the rewritable transient metamaterial permits realization of optical elements that change their properties on a shot-to-shot basis. Such modulation would be useful for the rapid generation of a series of superchiral fields³³ for sensing biomolecules³⁴ and chiral molecules.³⁵ Similarly, one could also cycle the phase in a pair of THz pulses to conduct low-noise two-dimensional spectroscopy at THz frequencies, as is already routinely performed in the mid-infrared regime.³⁶

ACKNOWLEDGMENTS

We would like to thank the German Research Foundation for funding this work through Grant No. KA 3305/2-1.

- 1 Tonouchi M. Cutting-edge terahertz technology. *Nat Photon* 2007; **1**: 97–105.
- 2 Ulbricht R, Hendry E, Shan J, Heinz TF, Bonn M. Carrier dynamics in semiconductors studied with time-resolved terahertz spectroscopy. *Rev Mod Phys* 2011; **83**: 543–586.
- 3 Hoffmann MC. Nonlinear terahertz spectroscopy. In: Peiponen KE, Zeitler A, Kuwata-Gonokami M, editors. *Terahertz Spectroscopy and Imaging*. Vol. 171. Berlin: Springer Series in Optical Sciences; 2013. pp355–388.
- 4 Chan WL, Deibel J, Mittleman DM. Imaging with terahertz radiation. *Rep Prog Phys* 2007; **70**: 1325–1379.
- 5 Federici J, Moeller L. Review of terahertz and subterahertz wireless communications. *J Appl Phys* 2010; **107**: 111101.
- 6 Vidal S, Degert J, Oberlé J, Freysz E. Femtosecond optical pulse shaping for tunable terahertz pulse generation. *J Opt Soc Am B* 2010; **27**: 1044–1050.
- 7 Scherger B, Scheller M, Vieweg N, Cundiff ST, Koch M. Paper terahertz waveplates. *Opt Express* 2011; **19**: 24884–24889.
- 8 Qi T, Shin YH, Yeh KL, Nelson KA, Rappe AM. Collective coherent control: synchronization of polarization in ferroelectric PbTiO_3 by shaped THz fields. *Phys Rev Lett* 2009; **102**: 247603.
- 9 Günther G, Anappara AA, Hees J, Sell A, Biasiol G *et al*. Sub-cycle switch-on of ultrastrong light–matter interaction. *Nature* 2009; **458**: 178–181.
- 10 Rahm M, Li JS, Padilla WJ. THz wave modulators: a brief review on different modulation techniques. *J Infrared Milli Terahz Waves* 2013; **34**: 1–27.
- 11 Hendry E, Garcia-Vidal FJ, Martin-Moreno L, Gómez Rivas J, Bonn M *et al*. Optical control over surface-plasmon-polariton-assisted THz transmission through a slit aperture. *Phys Rev Lett* 2008; **100**: 123901.
- 12 Chen HT, Padilla WJ, Zide JM, Gossard AC, Taylor AJ *et al*. Active terahertz metamaterial devices. *Nature* 2006; **444**: 597–600.
- 13 Berrier A, Ulbricht R, Bonn M, Gómez Rivas J. Ultrafast active control of localized surface plasmon resonances in silicon bowtie antennas. *Opt Express* 2010; **18**: 23226–23235.
- 14 Chen HT, O’Hara JF, Azad AK, Taylor AJ, Averitt RD *et al*. Experimental demonstration of frequency-agile terahertz metamaterials. *Nat Photon* 2008; **2**: 295–298.
- 15 Chen HT, Padilla WJ, Cich MJ, Azad AK, Averitt RD *et al*. A metamaterial solid-state terahertz phase modulator. *Nat Photon* 2009; **3**: 148–151.
- 16 Driscoll T, Kim HT, Chae BG, Kim BJ, Lee YW *et al*. Memory metamaterials. *Science* 2009; **325**: 1518–1521.
- 17 Chen HT, O’Hara JF, Azad AK, Taylor AJ. Manipulation of terahertz radiation using metamaterials. *Laser Photonics Rev* 2011; **5**: 513–533.
- 18 Rotenberg N, Betz M, van Driel HM. Ultrafast all-optical coupling of light to surface plasmon polaritons on plain metal surfaces. *Phys Rev Lett* 2010; **105**: 017402.

- 19 Okada T, Ooi K, Nakata Y, Fujita K, Tanaka K *et al*. Direct creation of a photoinduced metallic structure and its optical properties in the terahertz frequency region. *Opt Lett* 2010; **35**: 1719–1721.
- 20 Busch S, Scherger B, Scheller M, Koch M. Optically controlled terahertz beam steering and imaging. *Opt Lett* 2012; **37**: 1391–1393.
- 21 Okada T, Tanaka K. Photo-designed terahertz devices. *Sci Rep* 2011; **1**: 121.
- 22 Jepsen PU, Schairer W, Libon IH, Lemmer U, Hecker NE *et al*. Ultrafast carrier trapping in microcrystalline silicon observed in optical pump-terahertz probe measurements. *Appl Phys Lett* 2001; **79**: 1291–1293.
- 23 Li CM, Sjodin T, Dai HL. Photoexcited carrier diffusion near a Si(111) surface: non-negligible consequence of carrier–carrier scattering. *Phys Rev B* 1997; **56**: 15252–15255.
- 24 Beggs DM, Krauss TF, Kuipers L, Kampfrath T. Ultrafast tilting of the dispersion of a photonic crystal and adiabatic spectral compression of light pulses. *Phys Rev Lett* 2012; **108**: 033902.
- 25 Lalanne P, Hutley M. The optical properties of artificial media structured at a subwavelength scale. In: Steed J, editor. *Encyclopedia of Optical Engineering*. New York: Dekker Publishing; 2003. pp62–71.
- 26 Born M, Wolf E. *Principles of Optics*. 4th ed. Oxford: Pergamon Press; 1970.
- 27 Hendry E, Koeberg M, Pijpers J, Bonn M. Reduction of carrier mobility in semiconductors caused by charge–charge interactions. *Phys Rev B* 2007; **75**: 233202.
- 28 Waldow M, Plötzing T, Gottheil M, Först M, Bolten J *et al*. 25ps all-optical switching in oxygen implanted silicon-on-insulator microring resonator. *Opt Express* 2008; **16**: 7693–7702.
- 29 Först M, Manzoni C, Kaiser S, Tomioka Y, Tokura Y *et al*. Nonlinear phononics as an ultrafast route to lattice control. *Nat Phys* 2011; **7**: 854–856.
- 30 Fleischer S, Zhou Y, Field RW, Nelson KA. Molecular orientation and alignment by intense single-cycle THz pulses. *Phys Rev Lett* 2011; **107**: 163603.
- 31 Kampfrath T, Sell A, Klatt G, Pashkin A, Mährlein S *et al*. Coherent terahertz control of antiferromagnetic spin waves. *Nat Photon* 2011; **5**: 31–34.
- 32 Upham J, Tanaka Y, Asano T, Noda S. On-the-fly wavelength conversion of photons by dynamic control of photonic waveguides. *Appl Phys Express* 2010; **3**: 062001.
- 33 Davis TJ, Hendry E. Superchiral electromagnetic fields created by surface plasmons in nonchiral metallic nanostructures. *Phys Rev B* 2013; **87**: 085405.
- 34 Hendry E, Carpy T, Johnston J, Popland M, Mikhaylovskiy RV *et al*. Ultrasensitive detection and characterization of biomolecules using superchiral fields. *Nat Nanotechnol* 2010; **5**: 783–787.
- 35 Tang Y, Cohen AE. Enhanced enantioselectivity in excitation of chiral molecules by superchiral light. *Science* 2011; **332**: 333–336.
- 36 Xiong W, Laaser JE, Mehlenbacher RD, Zanni MT. Adding a dimension to the infrared spectra of interfaces using heterodyne detected 2D sum-frequency generation (HD 2D SFG) spectroscopy. *Proc Natl Acad Sci USA* 2011; **108**: 20902–20907.



This work is licensed under a Creative Commons Attribution-NonCommercial-ShareAlike 3.0 Unported license. To view a copy of this license, visit <http://creativecommons.org/licenses/by-nc-sa/3.0>

Supplementary Information for this article can be found on the *Light: Science & Applications*' website (<http://www.nature.com/lsa/>).